



ORIGINAL ARTICLE

In Silico Activity of AS1411 Aptamer Against Nucleolin of Cancer Cells

Zohreh Farahbakhsh¹, Mohammad Reza Zamani², Mohammad Rafienia^{3*}, Oğuz Gülseren⁴,
Mahmoud Mirzaei^{3*}

¹NourDanesh Institute of Higher Education, Meymeh, Iran

²National Institute of Genetic Engineering and Biotechnology (NIGEB), Tehran, Iran

³Biosensor Research Center, School of Advanced Technologies in Medicine, Isfahan University of Medical Sciences, Isfahan, Iran

⁴Department of Physics, Bilkent University, Ankara, Turkey

ARTICLE INFO

Article History:

Received: 12.05.2020

Accepted: 18.07.2020

Keywords:

Aptamer

AS1411

AT11

Nucleolin

In Silico

*Corresponding author:

Biosensor Research Center, School of
Advanced Technologies in Medicine,
Isfahan University of Medical
Sciences, Isfahan, Iran

Tel: +98-9034073500

Mohammad Rafienia,

Email: m_rafienia@med.mui.ac.ir,

Mahmoud Mirzaei,

Email: mdmirzaei@pharm.mui.ac.ir

ABSTRACT

Background: It has been expected that AS1411 aptamer could work against the cancer cells. Although the general information is available, there is still lack of details for the purpose. Therefore, activity of AS1411 aptamer against the nucleolin (NCL) target of cancer cells has been investigated in current work at the molecular scale. In addition, the same features have been also investigated for examining the activity of AT11, one of AS1411 derivatives.

Methods: This work has been done employing *in silico* Molecular Docking simulations. Ten starting 3D configurations have been considered for each aptamer to be docked against the NCL target. Conformational search processes of ligands against the target indicated that the starting configuration of ligand could play an important role in determining the final complex formation in both of quantitative and qualitative aspects.

Results: A04 and B01 are those starting configurations of AS1411 and AT11 making the strongest complexes with the NCL target among other ligands. The analyses indicated that the complexes of AT11 are slightly stronger than those of AS1411, in which the NCL target structure is more involved in the chelated complexes with the AT11 in comparison with the AS1411.

Conclusion: AS1411 and AT11 are specified for targeting the NCL of cancer cells for the diagnosis and therapeutic purposes. They have reasonable binding affinity and could work as possible inhibitors of NCL.

Please cite this article as: Farahbakhsh Z, Zamani MR, Rafienia M, Gülseren O, Mirzaei M. *In Silico* Activity of AS1411 Aptamer Against Nucleolin of Cancer Cells. IJBC 2020; 12(3): 95-100.

Introduction

Cancer has been seen as one of the serious problems to the health quality of people all around the world for several years.¹ Although the conventional therapeutics such as chemotherapy and surgery have been improved for better treatments of patients, but the problem is still remained unsolved.² Besides, unwanted side effects could suffer the patients after using such treatments.³ Therefore, considerable efforts have been dedicated to find possible solutions for developing more efficient protocols of cancer therapy.⁴ To this aim, knowledge about details of mechanism of cancer growth prevention could help to reproduce novel therapeutics for this health problem.⁵

In the case of pharmacotherapy, conditions of ligand-target interactions in both quantitative and qualitative aspects are important to make a brighter decision about the efficacy of desired ligand for inhibiting of target activity.⁶ Such details could be very well recognized by employing the *in silico* methodologies on simulation of 3D structures of molecular counterparts of interacting systems using computer systems and softwares.⁷⁻¹⁴ The quantitative binding energy could reveal information about the strength of ligand-target complex formation whereas the spherical shape could show the corresponding molecular configurations of interacting counterparts.¹⁵ By the benefits of employing *in silico* methodologies,

AS1411, a nucleic acid aptamer, interacts with NCL with over-expression at the surface of cancer cells.¹⁶ Interestingly, NCL is located inside the nuclei and cytoplasm of non-malignant cells; however, it will be expressed abnormally at the cell surfaces of malignant cells.¹⁷ This characteristic behavior has introduced NCL as a tumor biomarker of cancer cells, which could be detected by AS1411.¹⁸ In recent years, properties such as high-affinity binding with specific targets, chemical flexibility and tissue penetrating capability, have attracted attentions of researchers to examine the efficacy of nucleic acid aptamers in drug delivery systems especially for cancer cell growth preventions.¹⁹ Among which, nucleic acid based AS1411 aptamer has been seen *in vivo* to have selectivity against cancer cells for therapeutic purposes.²⁰ Furthermore, a series of AS1411 aptamer derivatives including AT11, have been recognized by NMR structural analysis showing promising potential for developing anticancer ligands.²¹ AS1411 itself is a G-rich chain of nucleotides, in which it could be flexibly folded in different 3D shapes.²² Since the 3D configuration is one of the important influencing features of structure-activity relationship (SAR), it is an important task to analyze the effects of configuration of AS1411 on complex formation of ligand-target interacting systems with NCL.²³ Hereby, activity of different 3D configurations of AS1411 against NCL has been analyzed in this work employing the *in silico* methodologies.

In silico Molecular Docking (MD) simulations have been performed to examine the ligand-target complex formation of AS1411 against NCL. To this aim, 3D structures of each counterpart have been first obtained from the Protein Data Bank (AS1411: 2N3M and NCL: 2KRR) and then submitted to HDock server for performing MD simulations.^{24, 25} Ten 3D configurations have been assigned for AS1411 to be docked against NCL with 100 number of conformation search for each configuration (Table 1 and Figure 1). The nucleotide chain of AS1411 is (5'-GGTGGTGGTGGTTGTGGTGGTGG-3'), in which the chain of its AT11 derivative is

Results

Conformational analyses of each of ten initial 3D configurations of AS1411 ligand against the NCL target have been done by the MD simulations of HDock server to evaluate the interacting complexes (Figure 1). It is noted that based on the original 3D structure of AS1411 (PDB: 2N3M), ten possible configurations have been reported based on their rational stability. Hence, all of ten configurations have been considered as separated starting AS1411 ligands for the interacting complex formation with the NCL target. The HDock scores declare that the earlier hypothesis of this work to investigate the effects of structural configuration on the interacting process of AS1411 was true because of obtaining different values of binding energies for different starting configurations (Table 1) in addition to different conformational representation against the NCL target (Figure 1). A quick look at the panels of Figure 1 indicates that the starting configuration plays a dominant role for localizing the ligand at the target site, in which different ligands are binding with different sites of NCL. The quantitative HDock scores also approves that the strength of interacting complexes are different regarding different starting configurations of AS1411 ligands, in which A04 has been seen to form the complex with the highest strength among all ten complexes of AS1411-NCL. Examining the results of other complexes shows significant

Aptamer AS1411	HDOCK Scoring	Aptamer AT11	HDOCK Scoring
A01	-269.71	B01	-264.71
A02	-215.84	B02	-250.81
A03	-246.93	B03	-241.99
A04	-270.46	B04	-233.44
A05	-234.93	B05	-235.92
A06	-240.58	B06	-261.03
A07	-231.73	B07	-261.51
A08	-248.86	B08	-244.26
A09	-238.84	B09	-220.42
A10	-246.96	B10	-240.95

96

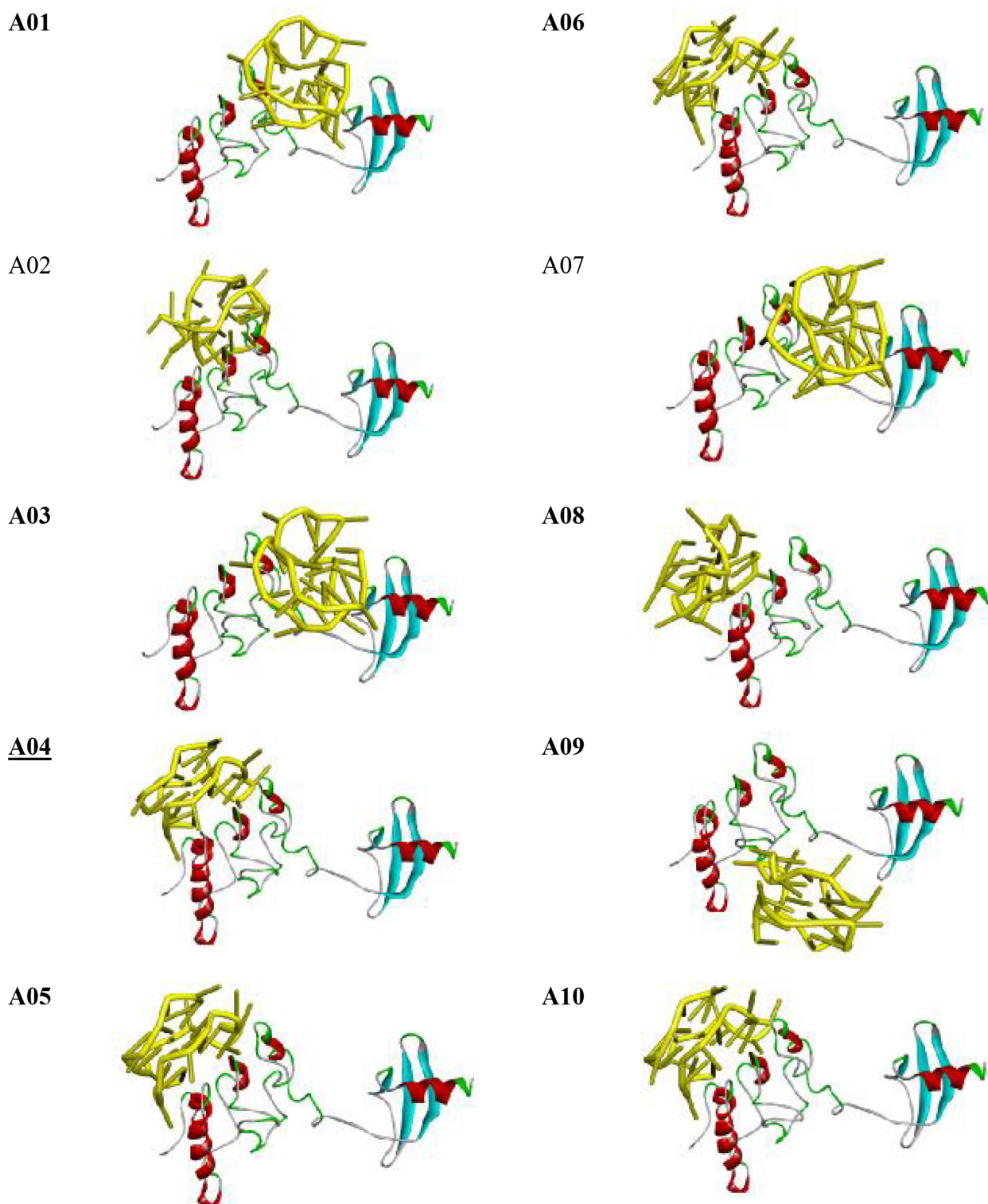


Figure 1: AS1411-NCL complexes regarding ten initial 3D configurations of AS1411. See Table 1 for more details.

differences for the obtained values of HDock scores, in which the score of A01 is only close to A04 and the strength orders for all complexes of different starting configurations are A04 > A01 > A08 A10 > A03 > A06 > A09 > A05 > A07 > A02. For showing molecular details of interactions in complexes, the NCL sequence could be divided into two left and right sites in Figure 1; the left site is [GSHMVEGSESTTPFNLFIGNLNPNS VAEKVAISELFAKNDLAVVDVRTGTNRKFGY VDFESAEDLEKALELTGLKVFGNEIKLEKPKG

RDSKKVRAARTLLAKNLSFNIT] and the right site is [EDELKEVFEDALEIRLVSQDGKSKGIAY IEFKSEADAENLEEKQGAIEDGRSVSLYYTGEK]. The results indicate that the ligands are mostly oriented to interact with the left site but with different binding strength. Very much interestingly, A04 interacts with NCL through its 5'-part (5'-GGTGGTGGTGGT) showing the highest strength but A02 interacts with NCL through its 3'-part (GTGGTGGTGGTGG-3') showing the lowest strength of complexes. By emphasizing again on the importance

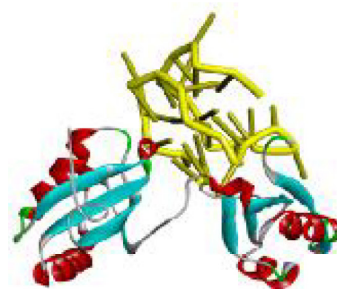
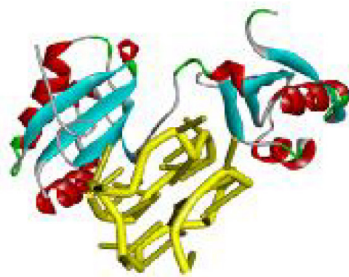
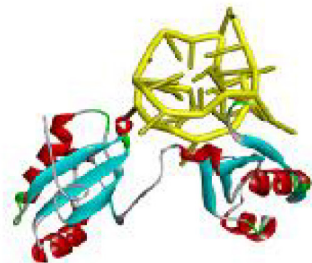
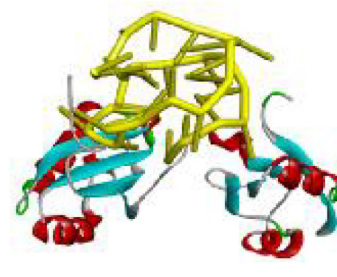
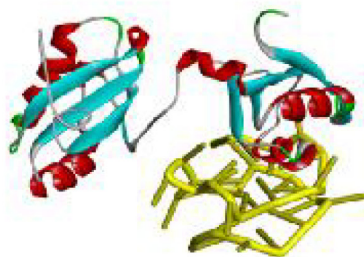
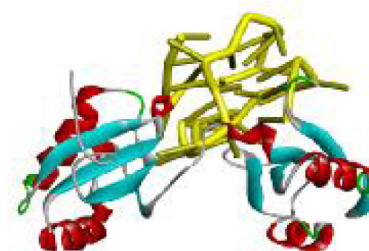
B01**B06****B02****B07****B03****B08****B04****B09****B05****B10**

Figure 2: AT11-NCL complexes regarding ten initial 3D configurations of AT11. See Table 1 for more details.

of starting configuration of ligand, the trend shows that it could orient the AS1411 how to relax at the target site, as could be clearly seen for A02 and A04 complexes. The same story has been seen for other A complexes, in which the 5'-part of AS1411 could make stronger complexes with NCL in comparison with the 3'-part.

AT11-NCL Complexes

For exploring efficacy of AS1411 derivative activity on interacting with the NCL target, the features of AT11

have been investigated and the resulted complexes have been compared with those of the original AS1411. Ten starting configurations have been employed in parallel with the configurations of the original AS1411, and the MD simulations with 100 numbers of conformational searching process have been performed to evaluate the formations of AT11-NCL complexes. The main difference between AS1411 and AT11 is additional of two T nucleotides; one T to beginning 5'-part and one T to ending 3'-part, besides replacement of one G of AS1411

by another T nucleotide (see Materials and Methods). The changes of aptamer building shows significant effects on the interactions of AT11 with the NCL target as presented in Figure 2 in comparison with Figure 1. Interestingly, the structural configuration of NCL also detects significant effects of AT11 presence in comparison with that of AS1411. By the obtained HDOCK scores, B01 shows the highest stability and B09 shows the lowest stability of AT11-NCL complexes, in which the stability order is $B01 > B07 > B06 > B02 > B08 > B03 > B10 > B05 > B04 > B09$. Comparing the average HDOCK scores indicates that the B complexes are slightly more stable than A complexes with the average score: -246 kcal/mol for B complexes and -244 kcal/mol for A complexes.

Discussion

Based on the importance of employing nucleic acid aptamers for cancer growth prevention, the activity of AS1411 against the NCL target has been investigated in this work employing the *in silico* MD simulations of interacting ligand-target complexes. Besides the original AS1411, AT11 has been also examined as one of derivatives with expected potency of interaction with the NCL target. Since the over-expression of NCL at the cell surface is a characteristic biomarker feature of cancer cells, aptamer binding with the NCL could have dual benefits of diagnosis and therapeutic for cancer problem. Therefore, knowing details of interacting aptamer-NCL complexes is important to be achieved *in silico*.

Since the performed MD simulation was flexible for both of ligand and target, slight changes of NCL structure could be observed for the complexes of the panels of Figure 1 for AS1411-NCL complexes. Avoiding the changes of each structural configuration, localization of AS1411 ligands at the NCL surface should be carefully considered for targeted drug deliver purposes and to improve the efficacy of employed treatment for the cancer diagnosis and therapeutic purposes. As an advantage of *in silico* investigations in comparison with experimental achievements, the localization of ligand at the target site could be recognized at the molecular scale in addition to its binding strength. Earlier investigations also indicated that the AS1411 is a proper ligand for binding with the NCL target but almost without details of importance of starting configuration and finalizing localization of ligand at the target site.³⁰ As a concluding remark of this part, it could be mentioned that the starting configurations of AS1411 is an important factor for assigning its activity against the NCL target with significant changes of binding energies of interacting complexes and the conformational localization of ligand at the target surface. The left site of NCL is a proper site for AS1411 to interact with, in which the 5'-part of aptamer is more proper for this purpose. And finally, such important configuration features should be considered for the targeted drug delivery purposes regarding the AS1411-NCL complexes.

The achievements of AT11-NCL complexes could mean that the activity of derivative has been slightly improve for more effective interaction with the NCL target, which is in agreement with the previous works introducing

AT11 as a proper ligand.¹⁴ Furthermore, Figure 2 represents that the AT11 is almost chelated by the NCL meaning that all structure of target is almost involved with the interacting ligand to make a chelated complex. Comparing with Figure 1, the target NCL structure was still free of influence of interacting AS1411 ligand in the complexes but this trend is more complicated for AT11 by re-configuration of the NCL sequence to make complexes. For drug delivery purposes, it could be mentioned that the dosage consumption of AT11 could be expected to be slightly lower than that of AS1411 based on the achievements in both of HDOCK scores and structural configurations. Molecular scale analyses show that in all cases the 5'-part of AT11 is involved in interactions with the NCL target in contrast with the obtained achievements about the 5'-part of AS1411 involving in strong and 3'-part involving in weak complex formations. As concluding remarks of this part, it could be mentioned that the AT11 derivative could work somehow better than the original AS1411 in both of quantitative and qualitative aspects regarding the achievements of AT11-NCL complexes.

Conclusion

Within this work, we have performed *in silico* MD simulations to investigate the activity of AS1411 aptamer against the NCL target of cancer cells. Besides, the same features have been also investigated for examining the activity of AT11, one of AS1411 derivatives. By the obtained results, some trends could be concluded. First, the starting configuration of aptamer is important for both of AS1411 and AT11 to make strong interactions with the NCL target. Second, overall strength of AT11 is slightly higher than AS1411 for complex formations with the NCL target. Third, 5'-part of AS1411 plays role of making stronger interactions with the NCL and 3'-part plays role of making weaker interactions whereas 5-part plays all roles in AT11 related complexes. Fourth, the NCL target is more involved in complexes with AT11 than AS1411. Fifth, the NCL target could be very well recognized by both of AT11 and AS1411 with higher overall efficacy for AT11. And finally, A04 and B01 are those aptamers specified for targeting the NCL of cancer cells for the diagnosis and therapeutic purposes.

Acknowledgements

The support of this work by the research council of Isfahan University of Medical Sciences under grant number 298096 and ethics code IR.MUI.RESEARCH.REC.1398.427 is acknowledged.

Conflict of Interest: None declared.

References

1. Siegel RL, Miller KD, Jemal A. Cancer statistics, 2020. *CA Cancer J Clin.* 2020;70(1):7-30. doi: 10.3322/caac.21590. PubMed PMID: 31912902.
2. Riley RS, June CH, Langer R, Mitchell MJ. Delivery technologies for cancer immunotherapy. *Nat Rev Drug Discov.* 2019;18(3):175-96. doi: 10.1038/s41573-018-0006-z.

3. Pearman TP, Beaumont JL, Mroczek D, O'Connor M, Cella D. Validity and usefulness of a single-item measure of patient-reported bother from side effects of cancer therapy. *Cancer*. 2018;124(5):991-7. doi: 10.1002/encr.31133. PubMed PMID: 29131323.
4. Schirrmacher V. From chemotherapy to biological therapy: A review of novel concepts to reduce the side effects of systemic cancer treatment. *Int J Oncol*. 2019;54(2):407-19. doi: 10.3892/ijo.2018.4661. PubMed PMID: 30570109. PubMed Central PMCID: PMC6317661.
5. Zuo Y, Pu J, Chen G, Shen W, Wang B. Study on the activity and mechanism of skimmianine against human non-small cell lung cancer. *Nat Prod Res*. 2019;33(5):759-62. doi: 10.1080/14786419.2017.1408096.
6. Tsai YT, Liang CH, Yu JH, Huang KC, Tung CH, Wu JE, et al. A DNA aptamer targeting galectin-1 as a novel immunotherapeutic strategy for lung cancer. *Mol Ther Nucleic Acids*. 2019; 18:991-8. doi: 10.1016/j.omtn.2019.10.029. PubMed PMID: 31778957.
7. Mirzaei M. Science and engineering in silico. *Adv J Sci Eng*. 2020;1(1):1-2. doi: 10.22034/AJSE2011001.
8. Partovi T, Mirzaei M, Hadipour NL. The C–H... O Hydrogen bonding effects on the 17o electric field gradient and chemical shielding tensors in crystalline 1-methyluracil: A DFT study. *Zeitschrift für Naturforschung A*. 2006;61(7-8):383-8. doi: 10.1515/zna-2006-7-812.
9. Behzadi H, Hadipour NL, Mirzaei M. A density functional study of 17O, 14N and 2H electric field gradient tensors in the real crystalline structure of α -glycine. *Biophys Chem*. 2007;125(1):179-83. doi: 10.1016/j.bpc.2006.07.010.
10. Harismah K, Ozkendir OM, Mirzaei M. Lithium adsorption at the C20 fullerene-like cage: DFT approach. *Adv J Sci Eng*. 2020;1(3):74-9. doi: 10.22034/AJSE2013074.
11. Faramarzi R, Falahati M, Mirzaei M. Interactions of fluorouracil by CNT and BNNT: DFT analyses. *Adv J Sci Eng*. 2020;1(2):62-6. doi: 10.22034/AJSE.2012062.
12. Tahmasebi E, Shakerzadeh E. Potential application of B40 fullerene as an innovative anode material for Ca-ion batteries: In silico investigation. *Lab-in-Silico*. 2020;1(1):16-20.
13. Gunaydin S, Alcan V, Mirzaei M, Ozkendir OM. Electronic structure study of Fe substituted RuO2 semiconductor. *Lab-in-Silico*. 2020;1(1):7-10.
14. Harismah K, Mirzaei M. Steviol and Iso-Steviol vs. Cyclooxygenase enzymes: In silico approach. *Lab-in-Silico*. 2020;1(1):11-5.
15. Harismah K, Mirzaei M. In silico interactions of steviol with monoamine oxidase enzymes. *Lab-in-Silico*. 2020;1(1):3-6.
16. Soundararajan S, Chen W, Spicer EK, Courtenay-Luck N, Fernandes DJ. The nucleolin targeting aptamer AS1411 destabilizes Bcl-2 messenger RNA in human breast cancer cells. *Cancer Res*. 2008;68(7):2358-65. doi: 10.1158/0008-5472.CAN-07-5723. PubMed PMID: 18381443.
17. Mongelard F, Bouvet P. Nucleolin: a multiFACeTed protein. *Trends Cell Biol*. 2007;17(2):80-6. doi: 10.1016/j.tcb.2006.11.010. PubMed PMID: 17557503.
18. Figueiredo J, Lopes-Nunes J, Carvalho J, Antunes F, Ribeiro M, Campello MP, et al. AS1411 derivatives as carriers of G-quadruplex ligands for cervical cancer cells. *Int J Pharm*. 2019; 568:118511. doi: 10.1016/j.ijpharm.2019.118511.
19. Vandghanooni S, Barar J, Eskandani M, Omidi Y. Aptamer-conjugated mesoporous silica nanoparticles for simultaneous imaging and therapy of cancer. *Trends Analyt Chem*. 2019;115759. doi: 10.1016/j.trac.2019.115759.
20. Jiang L, Wang H, Chen S. Aptamer (AS1411)-conjugated liposome for enhanced therapeutic efficacy of miRNA-29b in ovarian cancer. *J Nanosci Nanotechnol*. 2020;20(4):2025-31. doi: 10.1166/jnn.2020.17301.
21. Do NQ, Chung WJ, Truong TH, Heddi B, Phan AT. G-quadruplex structure of an anti-proliferative DNA sequence. *Nucleic Acids Res*. 2017;45(12):7487-93. doi: 10.1093/nar/gkx274. PubMed PMID: 28549181. PubMed Central PMCID: PMC5499593.
22. Bagheri Z, Ranjbar B, Latifi H, Zibaii MI, Moghadam TT, Azizi A. Spectral properties and thermal stability of AS1411 G-quadruplex. *Int J Biol Macromol*. 2015; 72:806-11. doi: 10.1016/j.ijbiomac.2014.09.016.
23. Zhang W, Xu P, Zhang H. Pectin in cancer therapy: a review. *Trends Food Sci Technol*. 2015;44(2):258-71. doi: 10.3389/fnut.2019.00072.
24. Berman HM, Westbrook J, Feng Z, Gilliland G, Bhat TN, Weissig H, et al. The protein data bank. *Nucleic Acids Res*. 2000;28(1):235-42. doi: 10.1093/nar/28.1.235.
25. Yan Y, Zhang D, Zhou P, Li B, Huang SY. HDock: a web server for protein–protein and protein–DNA/RNA docking based on a hybrid strategy. *Nucleic Acids Res*. 2017;45(W1):365-73. doi: 10.1093/nar/gkx407.
26. Emami N, Pakchin PS, Ferdousi R. Computational predictive approaches for interaction and structure of aptamers. *J Theor Biol*. 2020;110268. doi: 10.1016/j.jtbi.2020.110268.
27. Mirzaei M, Harismah K, Da'i M, Salarrezaei E, Roshandel Z. Screening efficacy of available HIV protease inhibitors on COVID-19 protease. *J Mil Med*. 2020; 22(2): 100-7
28. Ghanadian M, Ali Z, Khan IA, Balachandran P, Nikahd M, Aghaei M, et al. A new sesquiterpenoid from the shoots of Iranian *Daphne mucronata* Royle with selective inhibition of STAT3 and Smad3/4 cancer-related signaling pathways. *Daru*. 2020; 28(1):253-262. doi: 10.1007/s40199-020-00336-x
29. Ozkendir OM. Electronic Structure Study of Sn-Substituted InP Semiconductor. *Adv J Sci Eng*. 2020;1(1):7-11. doi: 10.22034/AJSE2011007.
30. Vivanco-Rojas O, García-Bermúdez MY, Iturriaga-Goyon E, Rebollo W, Buentello-Volante B, Magaña-Guerrero FS, et al. Corneal neovascularization is inhibited with nucleolin-binding aptamer, AS1411. *Exp Eye Res*. 2020; 193:107977. doi: 10.1016/j.exer.2020.107977.